INVESTIGATING CONTROL STRATEGIES FOR HAZARD MITIGATION OF COUPLED BUILDINGS

An Undergraduate Research Scholars Thesis

by

SHEYENNE DAVIS

Submitted to the Undergraduate Research Scholars program at
Texas A&M University
in partial fulfillment of the requirements for the designation as an

UNDERGRADUATE RESEARCH SCHOLAR

Approved by Research Advisor: Dr. Luciana Barroso

May 2020

Major: Civil Engineering

TABLE OF CONTENTS

ABSTRACT

Investigating Control Strategies for Hazard Mitigation of Coupled Buildings

Sheyenne Davis
Department of Civil and Environmental Engineering
Texas A&M University

Research Advisor: Dr. Luciana Barroso
Department of Civil and Environmental Engineering
Texas A&M University

In this research study, various control strategies for the hazard mitigation of coupled buildings during earthquakes are investigated, specifically the optimization of actuator location for a resettable spring semi-active device. Previous research has been done on which control strategies work best for coupled buildings during earthquakes, but there has not been anything definitive on an optimal actuator location. The foreseeable outcomes of this research are to determine the optimal actuator location based on structural control performance. Being able to optimize the actuator location will allow systems to run more efficiently and safely, which can make the use of semi-active devices for buildings more pragmatic.

ACKNOWLEDGMENTS

I would like to thank my advisor, Dr. Luciana Barroso, for helping me learn and guiding me through my research. I am also grateful to my friends and family, especially Mom and Dad, for their endless support. Lastly, thank you Ryan, for the encouragement and for acting interested when I talked about structural motion control.

NOMENCLATURE

[A]	State matrix
[B]	Input matrix
[C]	Output matrix
$[C_d]$	System damping matrix
[D]	Zero matrix
F(t)	Excitation force
{F(t)}	Excitation force vector
[I]	Identity matrix
[M]	System mass matrix
[K]	System stiffness matrix
k_s	Stiffness of spring
RMS	Root mean square
x_s	Unstretched length of spring
$x(t)$	Position
$\{x(t)\}$	Position vector
$\dot{x}(t)$	Velocity
$\{\dot{x}(t)\}$	Velocity vector
$\ddot{x}(t)$	Acceleration
$\{\ddot{x}(t)\}$	Acceleration vector
{z}	State vector
[0]	Matrix of zeros

CHAPTER I

INTRODUCTION

Motivation

In traditional structural design, a building is designed so that it has the strength to resist the loads that it will likely experience over its lifetime. However, it has been found that strength-based design has its limitations, one of which is its energy dissipation (Connor, 2003). During an earthquake, energy is dissipated through inelastic deformation of the building, which can be expensive to repair. This problem has led to the innovation of different design methods, including motion-based structural design. This approach focuses on motion-based design criteria and uses control devices to respond to the current loads a building is experiencing. This means that the structural response can dissipate the energy in different ways and be optimized.

Background

Through research in the field of motion-based design, it has been determined that structural performance can be improved by coupling adjacent buildings with control devices, especially for hazardous seismic and wind loads. These control devices use sensors to determine the load the building is experiencing and then mitigate the response of the building by producing opposing forces. The focus of this research is the mitigation of coupled buildings to the response to earthquakes.

Structural control systems can be separated into the four categories of passive, active, semi-active, and hybrid (Saaed, et al., 2015). Passive systems mitigate the response without using an external power source and develop control forces using the motion of the structure. Active systems utilize sensors to measure the excitation and response of the system to develop

control forces. This means that unlike passive systems, they are able to adapt to various conditions but require a large use of power that is not usually realistic for civil engineering applications. Semi-active systems have emerged as a way to get the benefit of adaptation that active systems have without the drawback of large power usage. Semi-active systems utilize both sensors and the motion of the structure to develop control forces with a small amount of power. Hybrid systems combine elements of these three types to create a customized system that works best for the project (Symans & Constantinou, 1999). For the purpose of this research, semi-active devices will be focused on as passive and active have been studied more in depth.

There are various control systems within these categories. One of particular interest is the resettable spring due to its differences with other prominent semi-active devices. Many of these devices, such as magnetorheological (MR) dampers and electrorheological (ER) dampers, vary the damping properties of the system while the resettable spring changes the stiffness properties in addition to adding energy dissipation (Al-Fahdawi et al., 2019). As shown in Figure 1 below, the resettable spring is made up of a piston, cylinder, and valve that connects the two sides of the cylinder. Within the cylinder is a liquid that is being compressed when the valve is closed, thus generating large resisting forces that can be approximated with a linear spring (Jabbari & Bobrow, 2002). When the valve opens, the energy in the fluid dissipates as it turns to heat. If the valve is opened and closed quickly, the energy dissipation is modeled as though the unstretched length of the spring is reset. The resettable spring can be modeled so it responds to certain events; therefore, if the valve is activated at the right time, the maximum amount of energy can be dissipated.

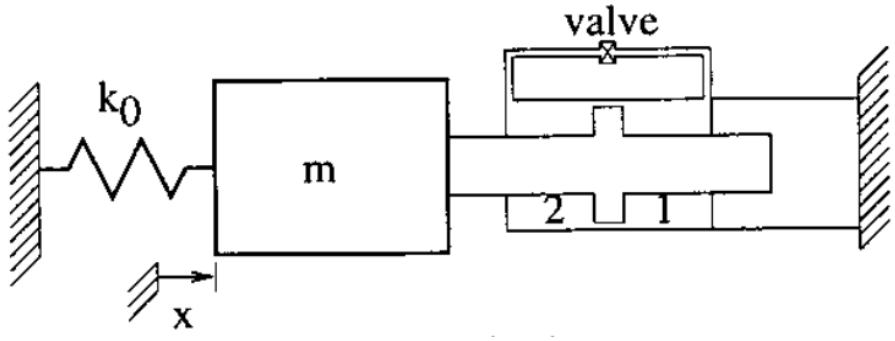

Figure 1. Resettable Spring Configuration (Jabbari & Bobrow, 2002)

A point of consideration in the research of structural motion control is which control algorithm will be used. Al-Fahdawi et al. (2019) considered this in the study of the use of simple adaptive control (SAC), where SAC was compared with Linear Quadratic Regulation (LQR). LQR is a traditional control algorithm that operates by generating an optimal feedback gain by minimizing a cost function that includes the state of the system and the force used to mitigate response. This is a simple method but is not very flexible. SAC is a control algorithm that utilizes a reference model that it tries to match, which makes it more flexible. Within this research, the resettable spring's control strategies will be examined.

The primary focus of this research is the use of a resettable spring to couple two buildings. Christenson et al. (2006) considered the effects of the configuration of the building and connector on the effectiveness of coupled building control. That research aimed to find the optimal location of the coupling link, but it only compared passive and active control systems and did not consider semi-active systems. Al-Fahdawi et al. (2019) tested various semi-active control systems with coupled buildings but focused more on the control method rather than the actual device.

Research Objectives

The main objective of this research is to determine the optimal location of a semi-active control device between coupled buildings, specifically a resettable spring, during earthquakes. Another objective is to determine the most effective control strategy and parameters that may impact that determination. In accomplishing these objectives, these systems will become safer and more efficient. It also continues research into semi-active control devices, which will hopefully lead to them becoming more prevalent in real structures.

CHAPTER II

METHODS

Building Models

MATLAB and Simulink were used to develop the simulation models that undergo the earthquake excitations. MATLAB handles the script portion of the code, which includes calculating constants and other characteristics of the building model. Simulink is a graphical program and simulates the building(s) undergoing the excitations.

This research was conducted in two phases: Phase 1, which looked at single buildings, and Phase 2, which looked at coupled buildings. Phase 1 consists of two models. The first is a simple, one-story building, shown in Figure 2a below. It is a single degree of freedom system, assumed to be a concrete slab with the following dimensions: 60 m x 30 m x 0.15 m. The mass is assumed to be concentrated in the center of the slab, and the actuator is placed so that it is parallel to the floor. The other Phase 1 model has three degrees of freedom and is similar to the first model, but just has three stories 4.5 m tall, as shown in Figure 2b. The actuator is placed on one floor of choice for each simulation to see which location is the most effective. The Phase 2 model for the coupled buildings was developed with two multi-story buildings, shown in Figure 3. It is assumed the floors are collinear and the actuator lays between one of the floors the buildings have in common. The actuator location is once again varied for each simulation to determine which is the most optimal.

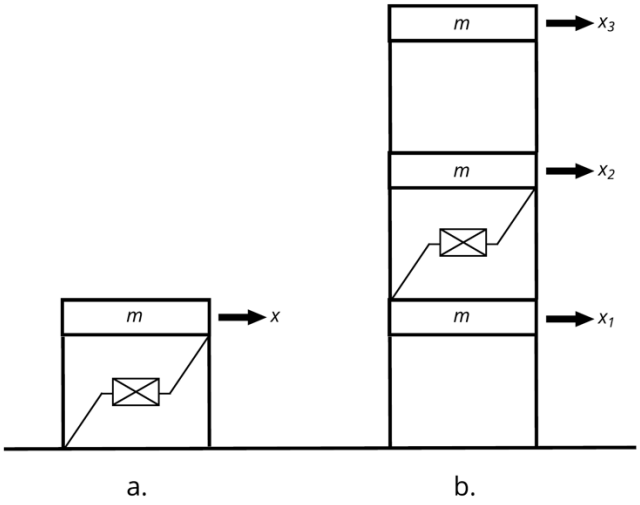

Figure 2. Phase 1 Single Building Models

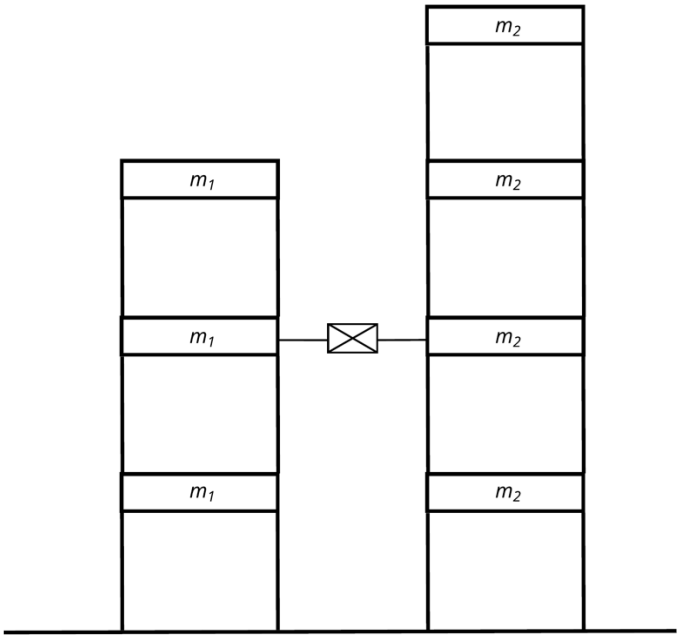

Figure 3. Phase 2 Coupled Buildings Model

The buildings are simulated under the excitations using state space modeling. This modeling acts in accordance with the following equation of motion:

$$[M]\{\ddot{x}(t)\} + [C_d]\{\dot{x}(t)\} + [K]\{x(t)\} = \{F(t)\} \quad (1)$$

where [M], [C_d], and [K] are the mass, damping, and stiffness matrices of the system; $\{\ddot{x}(t)\}, \{\dot{x}(t)\}$, and $\{x(t)\}$ are the acceleration, velocity, and position vectors of the system, and $\{F(t)\}$ is the force vector from the excitation. This equation can be rearranged to give the following equations:

$$\{\dot{z}\} = [A]\{z\} + [B]\{F(t)\} \quad (2)$$

$$\{y(t)\} = [C]\{z\} + [D]\{F(t)\} \quad (3)$$

where:

$$\{z\} = \begin{Bmatrix}\{x\}\\ \{\dot{x}\}\end{Bmatrix} \quad (4)$$

$$[A] = \begin{bmatrix}[0] & [I]\\ -[M]^{-1}[K] & -[M]^{-1}[C_d]\end{bmatrix} \quad (5)$$

$$[B] = \begin{bmatrix}[0]\\ [M]^{-1}\end{bmatrix} \quad (6)$$

$$[C] = [I] \quad (7)$$

$$[D] = [0] \quad (8)$$

and [I] is the identity matrix and [0] is a matrix of zeros, both the size of the number of degrees of freedom in the system.

For each floor, the density of concrete was used to calculate the mass of the slab. Each floor's mass does not affect the others, so the mass matrix of one building is then:

$$[M_1] = \begin{bmatrix} m & 0 & 0\\ 0 & \ddots & 0\\ 0 & 0 & m\end{bmatrix} \quad (9)$$

where m is the mass of one floor. The matrix will be square, and the size will correspond to the number of floors. The stiffness of each story was found by calculating it based off the buildings'

natural periods. The stiffness of each story affects the neighboring stories, so the stiffness matrix of one building is then:

$$[K_1] = \begin{bmatrix} 2k & -k & 0 & 0 \\ -k & 2k & \ddots & 0 \\ 0 & \ddots & \ddots & -k \\ 0 & 0 & -k & k \end{bmatrix} \tag{10}$$

where k is the stiffness of one story. Once again, the matrix will be square, and the size will correspond to the number of stories. The mass and stiffness matrices for the coupled system are the following:

$$[M] = \begin{bmatrix} [M_1] & [0] \\ [0] & [M_2] \end{bmatrix} \tag{11}$$

$$[K] = \begin{bmatrix} [K_1] & [0] \\ [0] & [K_2] \end{bmatrix} \tag{12}$$

where $[M_1]$ and $[K_1]$ correspond to the first building and $[M_2]$ and $[K_2]$ correspond to the second building. The damping values were found using modal analysis, so the matrix varies depending on the system. Modal analysis transforms the equation of motion into the modal space using eigenvectors, which uncouples the variables and allows for the damping values to be determined.

Control Strategies

The simulations run using the feedback loop shown in Figure 4 below. For each time step, the state space model is generated using equations 2 and 3. The solution to this system of differential equations is solved using an adaptive Runge-Kutta strategy implemented via MATLAB's ode45 solver. This will give the position and velocity of the building at that time based on the excitation forces. The program then uses the position and velocity of the building to calculate what force the resettable spring will produce, using the equation:

$$F_s = k_s x_s \tag{13}$$

where k_s is the stiffness of the spring and x_s is the unstretched length of the spring, initially zero. That force is then added to the force from the excitation for the next time step, and the process repeats.

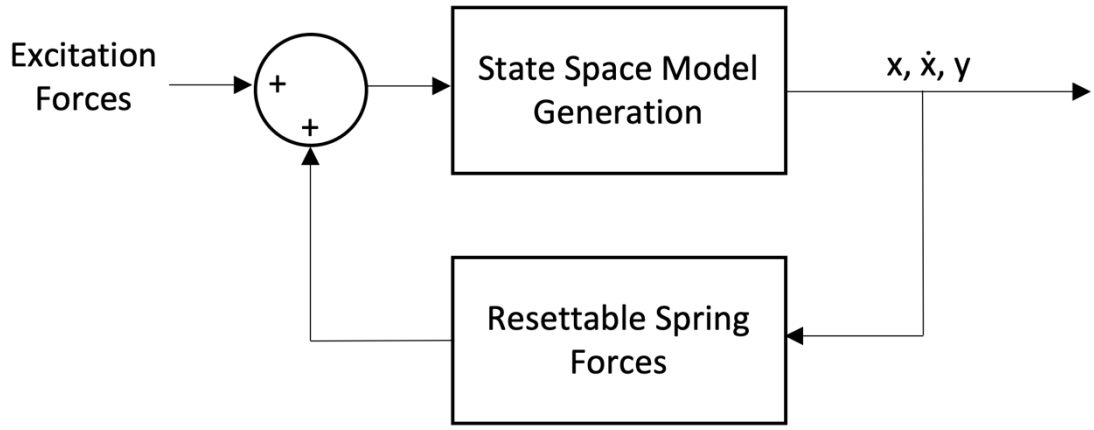

Figure 4. Building Model Simulation Feedback Loop

As mentioned previously, the resettable spring is an event-driven device that dissipates energy when its valve is quickly opened and closed, and its reset is represented by resetting the unstretched length of the spring to the current value of x. In order to maximize the amount of energy dissipated, the reset must occur when the spring is maximally stretched or compressed, or when the velocity is zero. However, the velocity almost never equals exactly zero due to the timestep of the simulation, so it is modeled in the resettable spring forces calculation by triggering the reset when the velocity changes signs. From there, x_s is set to equal the current position, x. This phenomenon is demonstrated in Figure 5, with Figure 5a corresponding to a normal spring and Figure 5b corresponding to a resettable spring. Figure 5a reveals the spring compressing and stretching like normal, with the graph traveling along one line over time. Figure 5b shows the resets on the vertical segments of the graph.

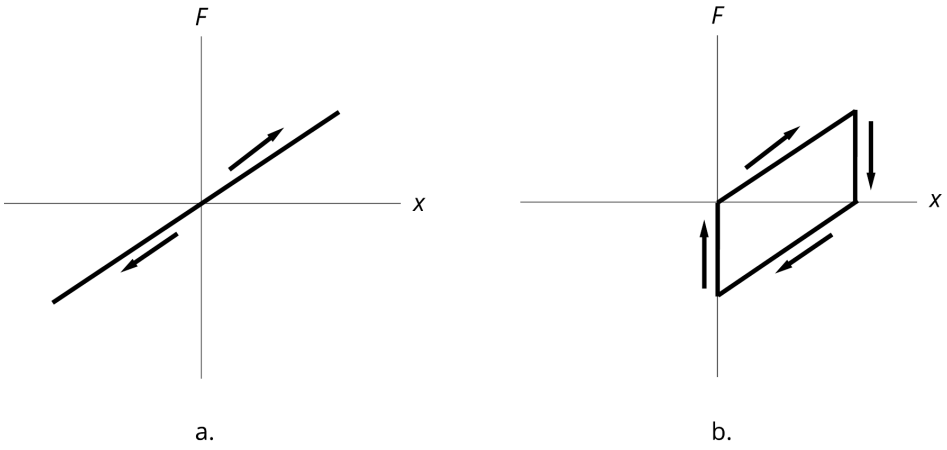

Figure 5. Spring Force v. Displacement

This control strategy becomes more complicated in the coupled buildings model as the device is connected to two different buildings and the force will be halved between them. Because the buildings have their own stiffness values, the force that the resettable spring outputs will be different for each building. This leads to the device being represented by two springs and introduces the question of what event will trigger the reset. The buildings are moving at two different velocities, so the choices are to consider both velocities separately (Two-Ended Velocity Method) or reset the spring when the relative velocity changes signs (Relative Velocity Method). In the Two-Ended Velocity Method, the reset is triggered when either velocity changes signs, but both unstretched spring lengths are reset. In the Relative Velocity Method, the reset is triggered when the relative velocity changes signs, and both unstretched spring lengths are reset. Both the Two-Ended Velocity Method and the Relative Velocity Method are tested to see which is the most effective control strategy.

Excitations

The buildings undergo a series of excitations. The first is a sine wave, with a period corresponding to the building's natural frequency. This corresponds to a resonance condition, a worst-case scenario for undamped systems. The other excitations are forces calculated from recorded accelerations from the earthquakes in El Centro in 1940, in Mexico City in 1985, and in Northridge in 1994. The uncontrolled building response to the excitations are shown in Figures 6 – 9 below. These earthquake suites were chosen due to some differences between them. El Centro's accelerations were recorded away from the epicenter of the earthquake while those in Northridge were recorded near the epicenter. Mexico City's soil is softer than that of El Centro or Northridge. As a result, these ground motions are characterized by widely different frequency content, allowing us to investigate the impact of the strategy under a wide range of conditions.

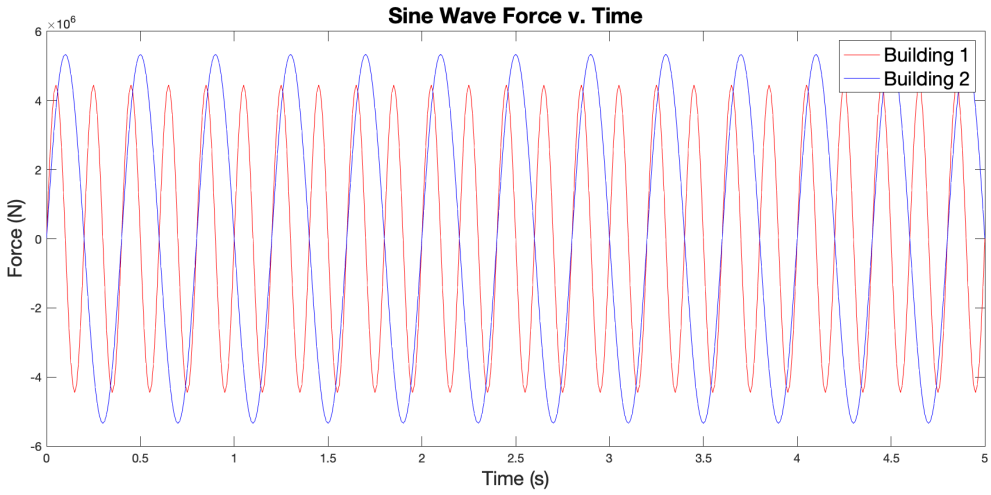

Figure 6. Uncontrolled Building Response to Sine Wave Excitation

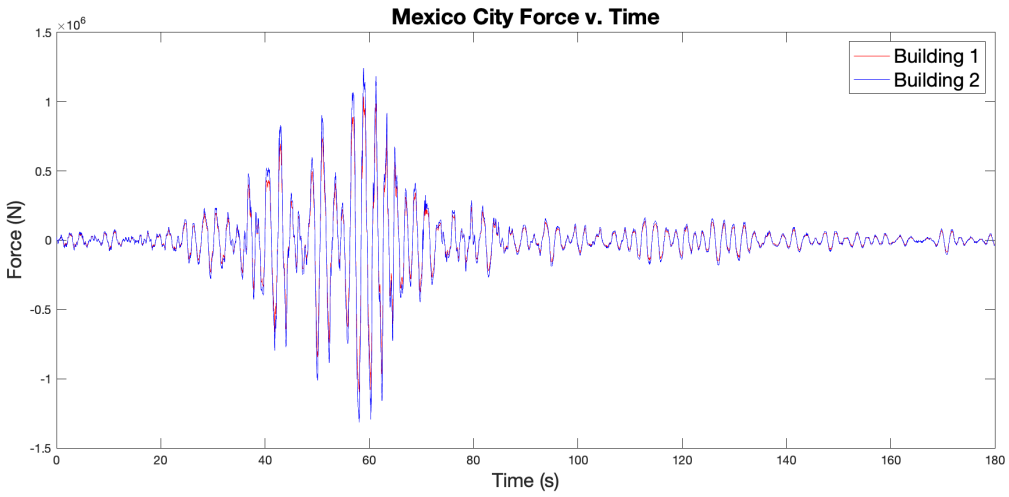

Figure 7. Uncontrolled Building Response to Mexico City Excitation

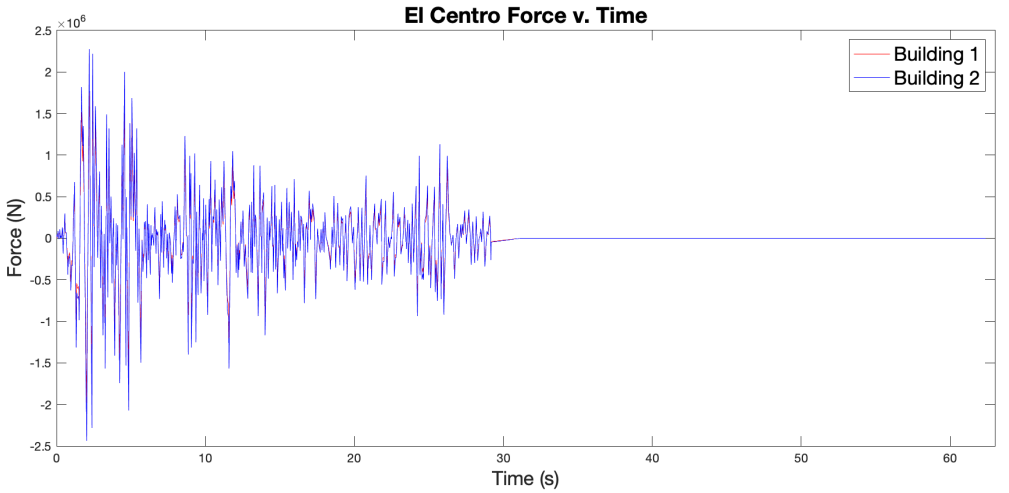

Figure 8. Uncontrolled Building Response to El Centro Excitation

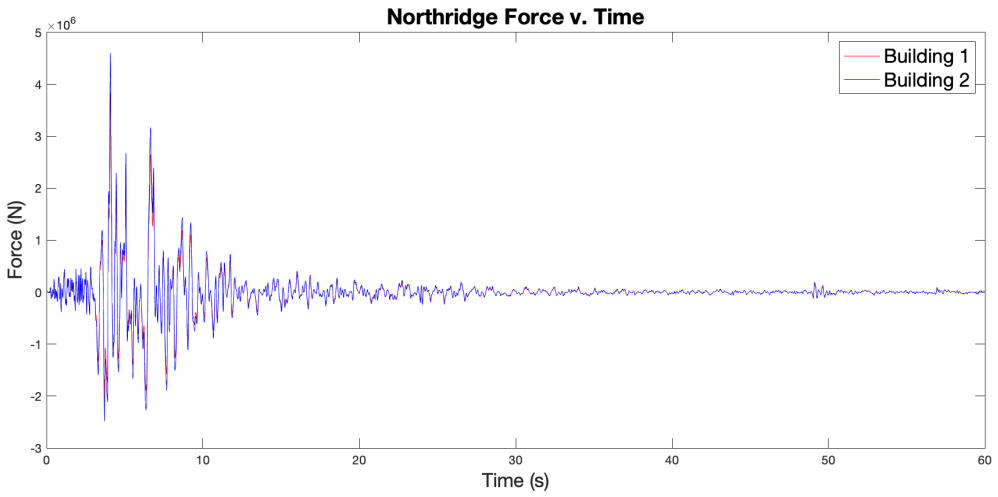

Figure 9. Uncontrolled Building Response to Northridge Excitation

CHAPTER III

RESULTS

Each simulation that is run outputs an enormous amount of data that gives the position of the building(s) at each time step for each configuration of the model. In order to determine the effectiveness of the resettable spring, the position data with no device will be compared to the data with each device configuration. The reduction in peak displacement, the root mean square of the displacement (RMS), and interstory drift ratio (where applicable) will be examined. Peak displacement reduction is a good indication of performance since part of the goal of using an actuator is to decrease the displacement a building experiences. The RMS will be taken of the difference between the two sets of data to give the average reduction in displacement over the entire simulation. Because this method does not account for which set of data is greater, only configurations with a positive peak displacement reduction will be used. Interstory drift is an important parameter to consider because it indicates the difference in movement between the floors. The interstory drift ratio is defined as the difference between the displacement of the two floors divided by the height between them. Typically, a ratio of greater than 5% is considered unacceptable and corresponds to structural failure of the building.

Phase 1: Single Building

One-Story Building

For the one-story building model, the only configuration possible is having the resettable spring on the first floor. Unlike the three-story building and coupled buildings models, it is not possible to determine an optimal actuator location since only one location is possible. Therefore,

these results will compare the model with and without the actuator for each excitation and consider the differences in effectiveness for the various excitations.

Since there would be nothing to compare the reduction with, the peak displacement rather than the peak displacement reduction is shown in Table 1, along with the percent decrease. For this simple model, the resettable spring reduces the peak displacement for each of the excitations. It was most effective for the sine wave excitation and least effective for the Mexico City earthquake.

Table 1. Peak Displacement of Single-Story Building

Excitation	With Actuator (m)	Without Actuator (m)	% Decrease
Sine Wave	0.0378	0.7789	95.15
Mexico City	0.0061	0.0064	4.68
El Centro	0.0102	0.0195	47.69
Northridge	0.0184	0.0468	60.68

The RMS of the difference in displacement is shown in Table 2. To give a reference as to what this average means, the RMS as a percentage of the peak difference is also given. The resettable spring is again shown to be most effective for the sine wave excitation and least effective for the Mexico City earthquake.

Table 2. Root Mean Square for Single-Story Building

Excitation	RMS (m)	% of Peak Difference
Sine Wave	0.05488	74.05
Mexico City	4.96E-4	12.71
El Centro	0.0041	33.88
Northridge	0.01	22.73

The significant reduction in both the sine wave's peak displacement and average displacement can also be observed in its time history shown in Figure 10. The effectiveness of the resettable spring on the sine wave excitation can most likely be attributed to its shape. Because the position greatly increases and maintains its peak throughout the simulation, there are

more opportunities for reduction than in the earthquakes where the position decreases as the earthquake nears its end.

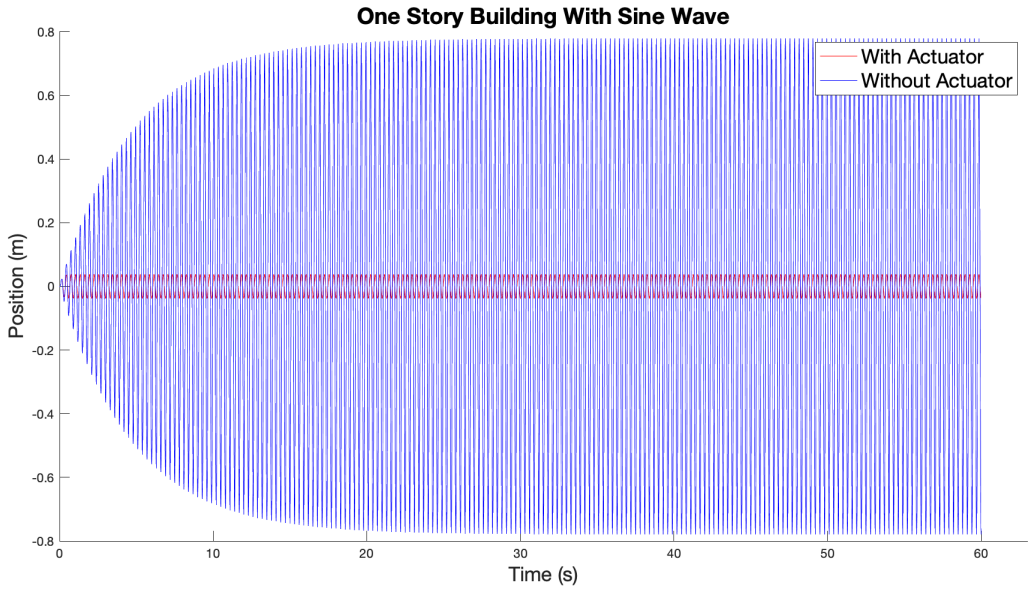

Figure 10. Position v. Time for One-Story Building with Sine Wave Excitation

Multiple-Story Building

For the three-story building model, the three possible configurations are putting the actuator on the first, second, or third floors. When the actuator was put on the third floor, the position of the building skyrocketed, meaning the resettable spring at this location is thoroughly ineffective. Therefore, only the configurations of the device being on the first or second floors will be considered. These configurations will be compared with each other to determine which floor is the optimal location for the resettable spring in one multi-story building. Since position data is only available from these three stories, the data for each story will be given along with an average.

The peak displacement reduction for each excitation is shown in Table 3. For each excitation except the sine wave, the more effective actuator location is highlighted in the table.

The sine wave's results did not vary much with a change in the actuator location. The second floor was found to be the optimal location for the El Centro and Northridge earthquakes while the first floor was optimal for the Mexico City earthquake. When the actuator was placed on the second floor for the Mexico City earthquake, there were small increases in peak displacement rather than reductions.

Table 3. Peak Displacement Reduction for Three-Story Building

Excitation	**Actuator Location**	**1st Floor (m)**	**2nd Floor (m)**	**3rd Floor (m)**	**Average (m)**
Sine Wave	1st Floor	0	-3.57E-05	0.0058	0.001921
	2nd Floor	0	0	0.0058	0.001933
Mexico City	1st Floor	0.0051	0.0158	0.0225	0.014467
	2nd Floor	-0.0015	-0.002	0.0082	0.001567
El Centro	1st Floor	0.0198	0.0312	0.035	0.028667
	2nd Floor	0.0211	0.046	0.0598	0.0423
Northridge	1st Floor	0.0026	0.0296	0.0377	0.0233
	2nd Floor	0.0242	0.0508	0.0745	0.049833

Table 4. Root Mean Square for Three-Story Building

Excitation	**Actuator Location**	**1st Floor (m)**	**2nd Floor (m)**	**3rd Floor (m)**	**Average (m)**
Sine Wave	1st Floor	0.0035	0.0059	0.0075	0.005633
	2nd Floor	0.0039	0.007	0.0097	0.006867
El Centro	1st Floor	0.0109	0.0191	0.0237	0.0179
	2nd Floor	0.0129	0.023	0.0286	0.0215
Northridge	1st Floor	0.0094	0.0168	0.0212	0.0158
	2nd Floor	0.0121	0.0221	0.0272	0.020467

The RMS of the difference in displacement is shown in Table 4. The Mexico City excitation was excluded since its peak displacement increased for one of the actuator locations, as previously shown in Table 3. The most effective actuator location is again highlighted in the table. From this data, the optimal location is shown to be the second floor for each excitation.

The interstory drift ratio reduction is shown in Table 5. This data reinforces that a second-floor actuator location is optimal for the El Centro and Northridge earthquakes while a first-floor location is optimal for the Mexico City earthquake. However, the first floor is now being shown as an optimal actuator location for the sine wave excitation, which is contrary to the root mean square data.

Table 5. Interstory Drift Ratio Reduction for Three-Story Building

Excitation	**Actuator Location**	**Between 1st and 2nd Floors (%)**	**Between 2nd and 3rd Floors (%)**	**Average (%)**
Sine Wave	1st Floor	0.15	0.21	0.18
	2nd Floor	-0.0654	0.15	0.04233
Mexico City	1st Floor	0.19	0.0912	0.14062
	2nd Floor	-0.1	0.0247E-02	-0.03765
El Centro	1st Floor	0.2	0.12	0.16
	2nd Floor	0.26	0.28	0.27
Northridge	1st Floor	0.24	0.0927	0.1663
	2nd Floor	0.43	0.18	0.305

A summary of the optimal actuator locations for each data analysis method is shown in Table 6. The sine wave excitation had an optimal location of either the first or second floor, the El Centro and Northridge earthquakes had optimal locations of the second floor, and the Mexico City earthquake had an optimal location of the first floor. These results are also reflected in Figures 11 – 14, which show the third-floor time histories of the most effective configuration for each excitation.

Table 6. Optimal Actuator Locations for Three-Story Building

Excitation	Peak Displacement Reduction	Root Mean Square	Interstory Drift Ratio Reduction	Overall
Sine Wave	1st or 2nd	2nd	1st	1st or 2nd
Mexico City	1st	N/A	1st	1st
El Centro	2nd	2nd	2nd	2nd
Northridge	2nd	2nd	2nd	2nd

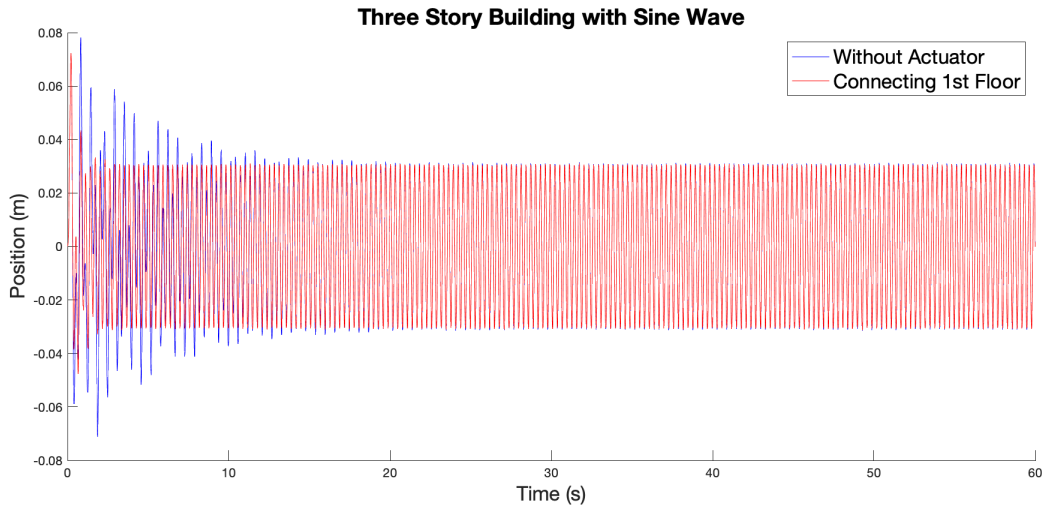

Figure 11. Position v. Time for Three-Story Building with Sine Wave Excitation

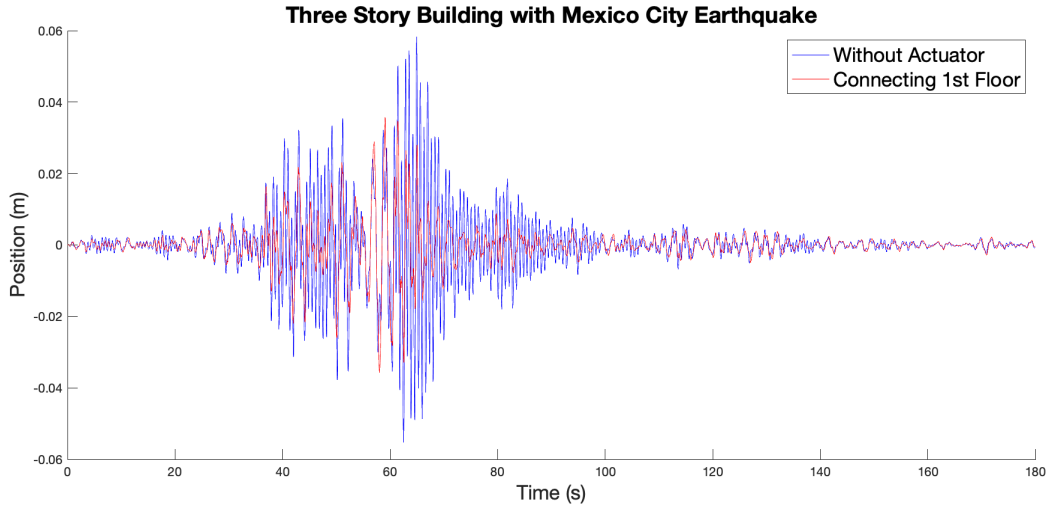

Figure 12. Position v. Time for Three-Story Building with Mexico City Earthquake

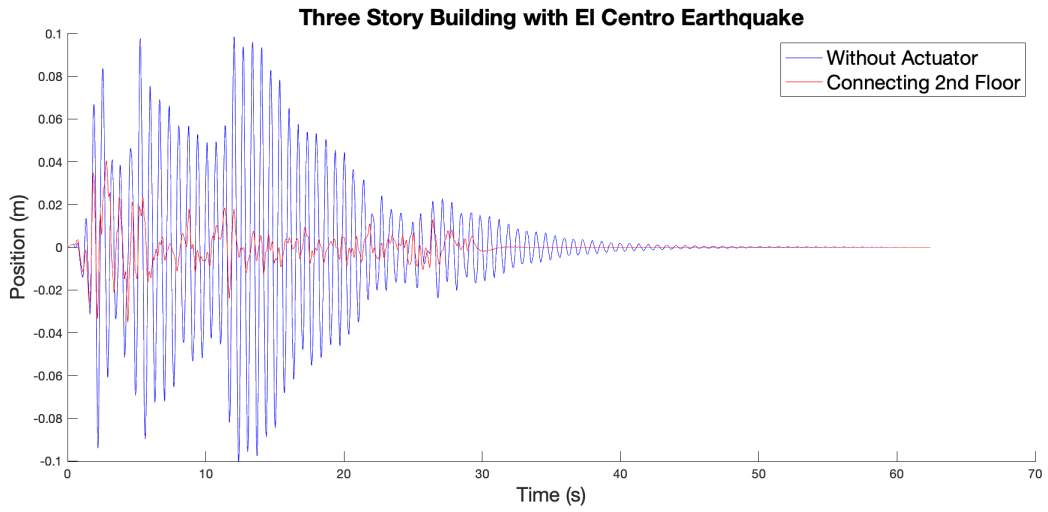

Figure 13. Position v. Time for Three-Story Building with El Centro Earthquake

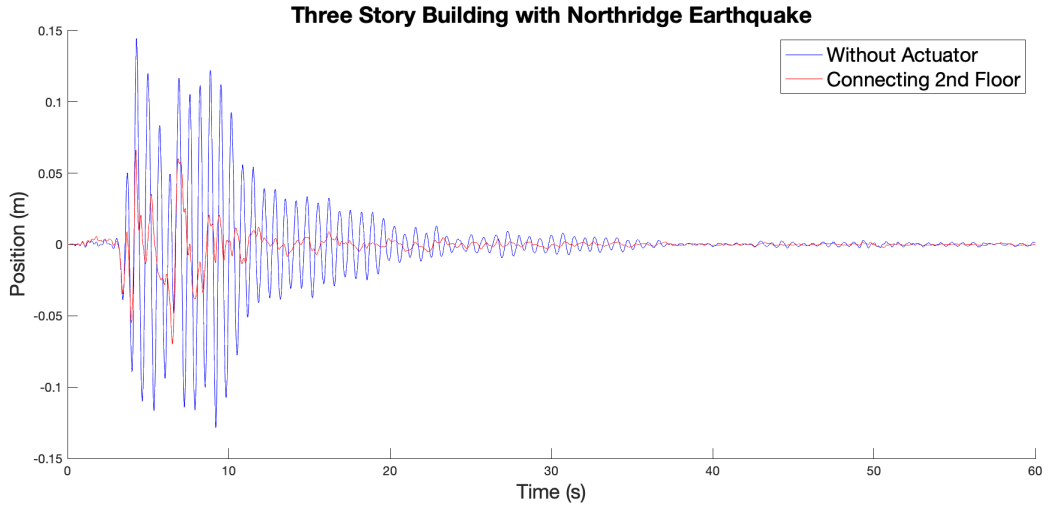

Figure 14. Position v. Time for Three-Story Building with Northridge Earthquake

Phase 2: Coupled Buildings

For the coupled buildings model with a three-story and four-story building, the three possible configurations are putting the actuator between the first, second, or third floors. The two control strategies being compared are the Two-Ended Velocity Method and the Relative Velocity Method. With position data for seven total floors, the average (μ) and average ± one standard deviation ($\mu \pm \sigma$) will be computed for the various result parameters.

The peak displacement reduction for each excitation and control method are shown in Table 7. All units are in meters. For each set of data, the Relative Velocity Method produced better results. The more effective actuator location is highlighted in the table for all excitations except the Mexico City earthquake. For the Mexico City earthquake, the peak displacement increased rather than decreased for each actuator location. The optimal device location was found to be the second floor for the sine wave excitation and El Centro earthquake while the Northridge earthquake had an optimal location of the third floor.

Table 7. Peak Displacement Reduction for Coupled Buildings

Excitation	**Actuator Location**	**Two-Ended Velocity Method**			**Relative Velocity Method**		
		$\mu - \sigma$	μ	$\mu + \sigma$	$\mu - \sigma$	μ	$\mu + \sigma$
Sine Wave	1st Floor	-0.0199	0.0815	0.183	-0.0226	0.0887	0.2
	2nd Floor	-0.0223	0.0842	0.1908	-0.0227	0.0905	0.2038
	3rd Floor	-0.0094	0.0034	0.0162	-0.0038	0.0037	0.0112
Mexico City	1st Floor	-0.0232	-0.0102	0.0028	-0.0074	-0.0029	0.0017
	2nd Floor	-0.0719	-0.0338	0.0044	-0.0103	-0.0029	0.0046
	3rd Floor	-0.124	-0.0578	0.0084	-0.0196	-0.0075	0.0047
El Centro	1st Floor	0.0062	0.0221	0.038	0.0058	0.0242	0.0425
	2nd Floor	0.0087	0.0355	0.0624	0.0123	0.0399	0.0675
	3rd Floor	0.0136	0.0292	0.0448	0.0144	0.0298	0.0453
Northridge	1st Floor	-0.0424	-0.0147	0.0129	-0.0306	-0.0073	0.0159
	2nd Floor	-0.0458	-0.0131	0.0197	-0.0206	0.0059	0.0325
	3rd Floor	-0.0069	0.0077	0.0224	0.0054	0.0202	0.035

The RMS of the difference in displacement is shown in Table 8. All units are in meters. The Two-Ended Velocity method produced better results for the El Centro and Northridge earthquakes while the Relative Velocity Method produced better results for the sine wave. This data reinforces the optimal actuator location is the second floor for the sine wave and the third floor for the Northridge earthquake. However, the optimal location for the El Centro earthquake for this data is now the third floor.

Table 8. Root Mean Square for Coupled Buildings

Excitation	Actuator Location	Two-Ended Velocity Method			Relative Velocity Method		
		μ - σ	μ	μ + σ	μ - σ	μ	μ + σ
Sine Wave	1st Floor	-0.0091	0.0687	0.1465	-0.0122	0.0781	0.1684
	2nd Floor	-0.0076	0.0692	0.1459	-0.0106	0.079	0.1685
	3rd Floor	0.002	0.0126	0.0233	0.004	0.0136	0.0232
El Centro	1st Floor	0.0075	0.0255	0.0435	0.0059	0.0214	0.0368
	2nd Floor	0.0108	0.029	0.0472	0.0094	0.0271	0.0447
	3rd Floor	0.0114	0.0298	0.0482	0.0104	0.0287	0.0471
Northridge	1st Floor	0.0085	0.0265	0.0445	0.007	0.022	0.0369
	2nd Floor	0.0122	0.032	0.0519	0.0106	0.0297	0.0488
	3rd Floor	0.0131	0.0353	0.0574	0.0118	0.032	0.0522

Table 9. Interstory Drift Ratio Reduction for Coupled Buildings

Excitation	Actuator Location	Two-Ended Velocity Method			Relative Velocity Method		
		μ - σ	μ	μ + σ	μ - σ	μ	μ + σ
Sine Wave	1st Floor	-0.63	1.9	4.44	-0.71	2.07	4.85
	2nd Floor	-0.77	1.97	4.71	-0.81	2.02	4.85
	3rd Floor	-0.0713	0.013	0.0973	-0.11	-0.0115	0.0885
Mexico City	1st Floor	-0.1	-0.0424	0.0198	-0.11	-0.0498	0.0134
	2nd Floor	-0.65	-0.28	0.0926	-0.26	-0.12	0.017
	3rd Floor	-1.23	-0.56	0.1	-0.34	-0.15	0.0352
El Centro	1st Floor	0.0404	0.16	0.27	0.026	0.16	0.3
	2nd Floor	0.11	0.27	0.42	0.14	0.32	0.49
	3rd Floor	0.0551	0.16	0.26	0.08	0.21	0.34
Northridge	1st Floor	-0.22	-0.0215	0.18	-0.0607	0.0472	0.16
	2nd Floor	-0.43	-0.0209	0.39	-0.17	0.0545	0.27
	3rd Floor	-0.39	-0.0838	0.22	-0.25	0.0604	0.37

The reduction in interstory drift ratio is shown in Table 9. All units are in %. The Relative Velocity Method produced better results for each set of data. The interstory drift ratio increased rather than decreasing for each configuration under the Mexico City earthquake. Once again, the third floor was shown to be the optimal location under the Northridge earthquake.

However, the sine wave had an optimal location of the first floor, and the El Centro earthquake had an optimal location of the second floor.

A summary of the optimal actuator locations is shown in Table 10. The optimal location for the sine wave excitation and El Centro earthquake was the second floor while the Northridge earthquake had an optimal location of the third floor. Interestingly, for the Mexico City earthquake, no actuator was optimal. These results are also reflected in Figures 15 – 17. Each figure shows the time histories of the most effective configuration for each excitation, excluding the Mexico City earthquake. The floor with the largest peak displacement reduction was chosen for each time history.

Table 10. Optimal Actuator Location for Coupled Buildings

Excitation	**Peak Displacement Reduction**	**Root Mean Square**	**Interstory Drift Ratio Reduction**	**Overall**
Sine Wave	2nd	2nd	1st	2nd
Mexico City	None	N/A	None	None
El Centro	2nd	3rd	2nd	2nd
Northridge	3rd	3rd	3rd	3rd

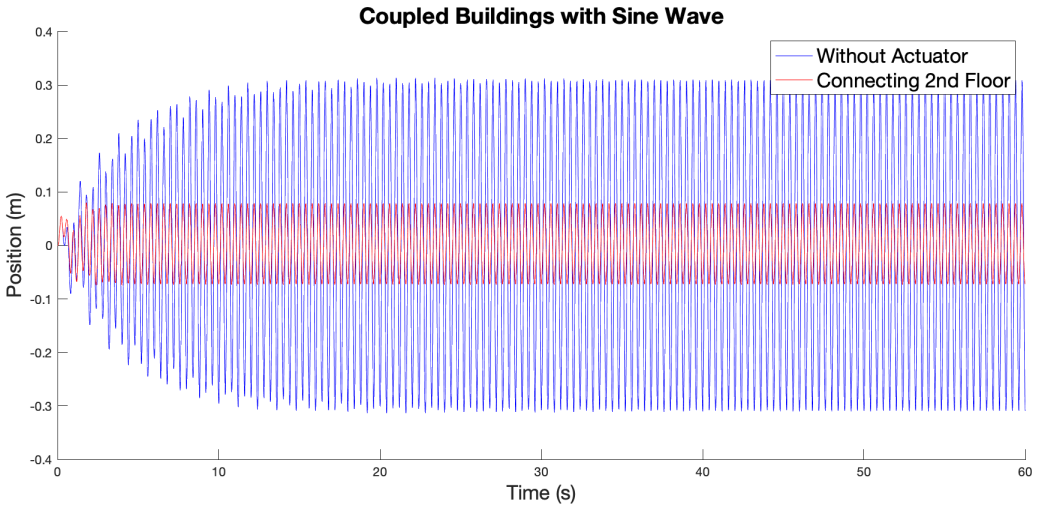

Figure 15. Position v. Time for Coupled Buildings with Sine Wave Excitation

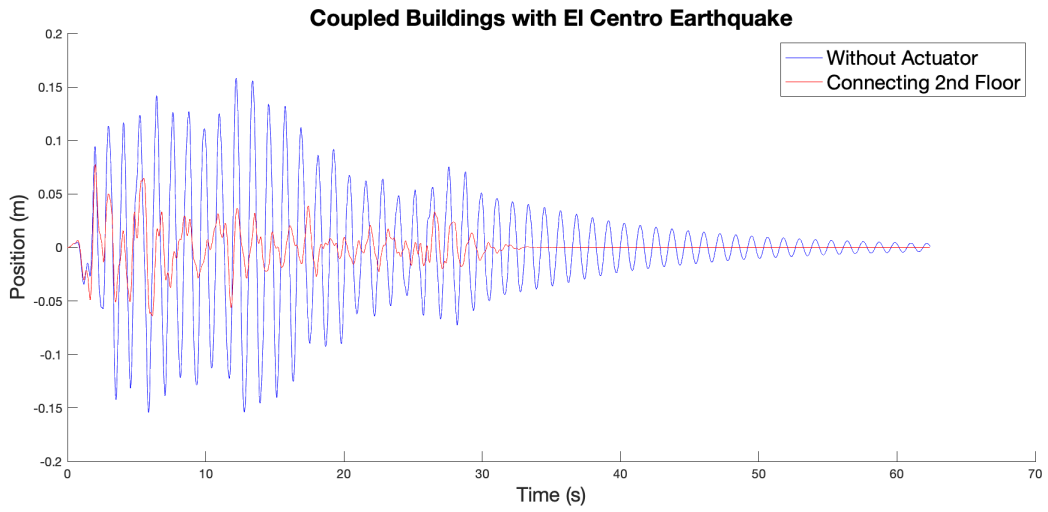

Figure 16. Position v. Time for Coupled Buildings with El Centro Earthquake

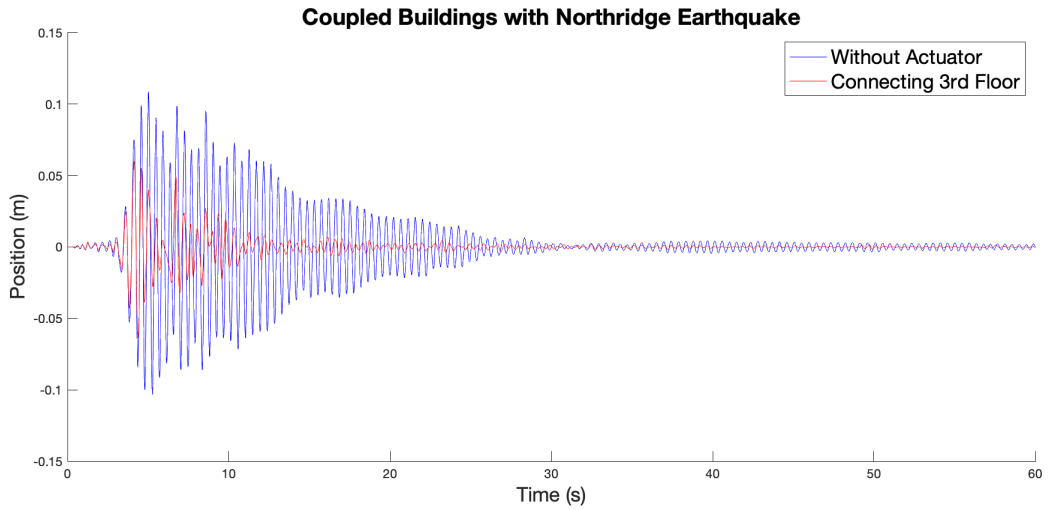

Figure 17. Position v. Time for Coupled Buildings with Northridge Earthquake

CHAPTER IV

CONCLUSION

The data in this research revealed that the resettable spring helps mitigate building response to earthquakes. It also determined the most effective actuator location and control strategy given each excitation. However, each earthquake is unique depending on factors such as location, soil type, and distance from the epicenter, which makes for different demands at each floor of each building. As such, future research is needed to determine how these varying factors influence the effectiveness of the resettable spring. Nevertheless, the resettable spring was overall effective and has potential as a semi-active control device.

Mexico City Earthquake

In each of the different models, the data from the Mexico City model was unexpected. For the single-story building, the resettable spring was much less effective in the Mexico City simulation than that of the other two earthquakes. For the three-story building, the optimal actuator location was found to be the first story under the Mexico City earthquake while the other two earthquakes had an optimal location of the second floor. Lastly, for the coupled building, there was no optimal actuator location under the Mexico City earthquake because each configuration made the building's response worse.

These results are interesting, and further investigation is needed to determine the cause. A possible source of these outcomes could be Mexico City's soft soil. When soil is soft, it amplifies the wave of the earthquake and can magnify the effects. It would be ideal for the resettable spring to work for different types of earthquakes in various locations, so additional research is

warranted to determine the reason for these results. Due to the inconsistencies, the Mexico City earthquake results will not be considered in any further conclusions.

Optimal Actuator Location

For the three-story building, the El Centro and Northridge earthquakes had optimal actuator locations of the second story while the sine wave excitation had an optimal location of either the first or second story. For the coupled buildings, the sine wave excitation and El Centro earthquakes had optimal actuator locations of the second floor while the Northridge earthquake had an optimal location of the third floor. It should be noted that for one of the tests the El Centro earthquake had an optimal location of the third floor.

These results are interesting because the actuator on the third floor of the three-story building proved ineffective, yet it works between the third floors of the coupled buildings. It appears that for both models, having the actuator on one of the middle floors works the best. This could be due to the fact that it is able to distribute the force the best from the middle of the building. However, if tested with taller buildings, it may be found that a middle floor closer to the top is a better optimal actuator location because it can better mitigate the more flexible building toward the top. It is difficult to tell with three and four-story buildings if the optimal actuator location is the true middle of the building or not. Therefore, more research is needed to come to a better conclusion.

Coupled Buildings Model Control Strategies

The Relative Velocity Method was found to be more effective than the Two-Ended Velocity Method. The Relative Velocity Method produced better results for all data when looking at peak displacement reduction and interstory drift reduction, and the Two-Ended Method only produced better results for most of the data when considering RMS. These results

are reasonable because considering the relative velocity takes into account the system as a whole rather than looking at the two buildings separately.

Future Work

Due to the various factors of the simulations run, there are many avenues for future work, but the main avenue is building more models. The next step is testing a resettable spring with taller buildings, such as a ten-story building. As buildings add more stories, they become more flexible, and it is imperative to determine how a resettable spring will work with a more flexible building under an excitation. The models outlined in this paper are relatively simple, so the models could be built with more complex features such as different methods of coupling buildings or looking at the differences between moment frames and braced frames.

Another channel for future research is the parameters of the models. As the models were built and the simulations were run, it became apparent the results changed depending on which building stiffness and period were used. These variables stayed constant for the purpose of this work, but it may be worth investigating how changing them affects the efficiency of the control device.

Lastly, sensor failure is an important part of structural motion control that should be explored. Due to power outages or other unexpected circumstances, the sensors in the control device may fail. If we can predict the response of buildings even with sensor failure, these control systems become safer and more practical for the future.

REFERENCES

Al-Fahdawi, O. A. S., Barroso, L. R., & Soares, R. W. (2019). Simple adaptive control method for mitigating the seismic responses of coupled adjacent buildings considering parameter variations. *Engineering Structures, 186*, 369-381. doi:10.1016/j.engstruct.2019.02.025

Christenson, R. E., Spencer, B. F., Johnson, E. A., & Seto, K. (2006). Coupled Building Control Considering the Effects of Building/Connector Configuration. *Journal of Structural Engineering, 132*(6), 853-863. doi:10.1061/(asce)0733-9445(2006)132:6(853)

Connor, J. J. (2003). Introduction to Structural Motion Control. Upper Saddle River, New Jersey: Peason Education, Inc.

Jabbari, F., & Bobrow, J. E. (2002). Vibration Suppression with Resettable Device. Journal of Engineering Mechanics, 128(9), 916-924. doi:10.1061/(asce)0733-9399(2002)128:9(916)

Saaed, T. E., Nikolakopoulos, G., Jonasson, J.-E., & Hedlund, H. (2015). A state-of-the-art review of structural control systems. *Journal of Vibration and Control, 21*(5), 919-937. doi:10.1177/1077546313478294

Symans, M. D., & Constantinou, M. C. (1999). Semi-active control systems for seismic protection of structures: a state-of-the-art review. *Engineering Structures, 21*(6), 469-487. doi:10.1016/s0141-0296(97)00225-3